

Interfacial reaction between Sn-rich solders and Ni-based metallization

M. He^a, A. Kumar^a, P.T. Yeo^a, G.J. Qi^b, Z. Chen^{a,*}

^aSchool of Materials Engineering, Nanyang Technological University, Nanyang Avenue, Singapore 639798, Singapore

^bSingapore Institute of Manufacturing Technology, 71 Nanyang Drive, Singapore 638075, Singapore

Available online 14 July 2004

Abstract

Solid state reaction between Sn-rich solders (Sn–3.5Ag and Sn–37Pb) and two types of Ni-based metallization (electroless Ni–P and sputtered Ni) has been studied. The growth rates of the main intermetallic compound (IMC), Ni₃Sn₄, at different aging temperatures are obtained and the activation energy calculated. Ni₃Sn₄ grows faster with Sn–3.5Ag solder than with Sn–37Pb solder under the same aging condition. The activation energy for the IMC growth with Ni–P metallization is higher than that with sputtered Ni metallization. Kirkendall voids are found inside Ni₃P layer after thermal aging in the solder/Ni–P UBM systems. This is the result of unbalanced element diffusion in solid state reaction between Sn-rich solders and Ni–P metallization. No voids are formed in solder/Ni system.

© 2004 Elsevier B.V. All rights reserved.

Keywords: Solder; Electroless nickel; Intermetallic compound; Thermal aging

1. Introduction

Historically Cr–Cu UBM was successfully used in the IBM C-4 technology where high lead content Sn–Pb solder was the bump material. Challenges surfaced when a similar flip chip structure was used for the chip-on-board applications where solders with low melting temperatures are necessary because of the low glass transition temperatures of the substrates. The most popular solder has been the eutectic tin–lead system that has a melting temperature of 183 °C [1,2]. Recently lead-free solders are used to replace the Pb-containing solders because of environmental concerns. A common feature of these low melting solders is their high Sn content, compared with the high-lead solder in the IBM C-4 technology. The solders were found to be not compatible with Cr–Cu under bump metallization (UBM) due to the effect of rapid spalling of Cu–Sn intermetallic compounds [3–6]. As alternatives, nickel-based UBMs, such as electroless Ni–P alloy (EN) and pure Ni either sputtered or electroplated, have attracted attention because of their fairly good wettability and slow reaction rate with solders [7,8]. Many studies have been devoted to the understanding of the interactions between

Sn-rich solders and Ni-based UBMs [9–12]. The information published so far shows it is still a concern, when using the nickel-based UBM with the popular tin-based solders (either lead-containing or lead-free). With different solder and UBM combinations, differences are expected in the types of intermetallic compounds formed, their morphology, and their growth rate under reflow and thermal aging conditions. All these correlate to their mechanical and electrical integrity.

In this paper, we present a comparison of the interaction of two Sn-containing solders (Sn–3.5Ag and eutectic Sn–Pb) with two types of nickel-based BUM (electroless Ni–P and sputtered Au/Ni). These materials were chosen based on the following considerations: Sn–3.5Ag solder is one of the popular lead-free solders and the eutectic Sn–Pb solder is still the most widely used materials in the industry. Ni–P UBM is gaining popularity because the simplicity (and thus low cost) of its manufacturing process. On the other hand, sputtered nickel is preferred in certain situations where a continuous film is required for bump build up by electroplating. A comparison among the four solder/UBM combinations would help understand the role of solder composition and UBM composition in the interfacial reaction. In this study, the morphology of intermetallic compound (IMC) formed under reflow and thermal aging conditions was observed. The IMC growth kinetics was assessed and compared.

* Corresponding author. Tel.: +65-67904256; fax: +65-67909081.
E-mail address: aszchen@ntu.edu.sg (Z. Chen).

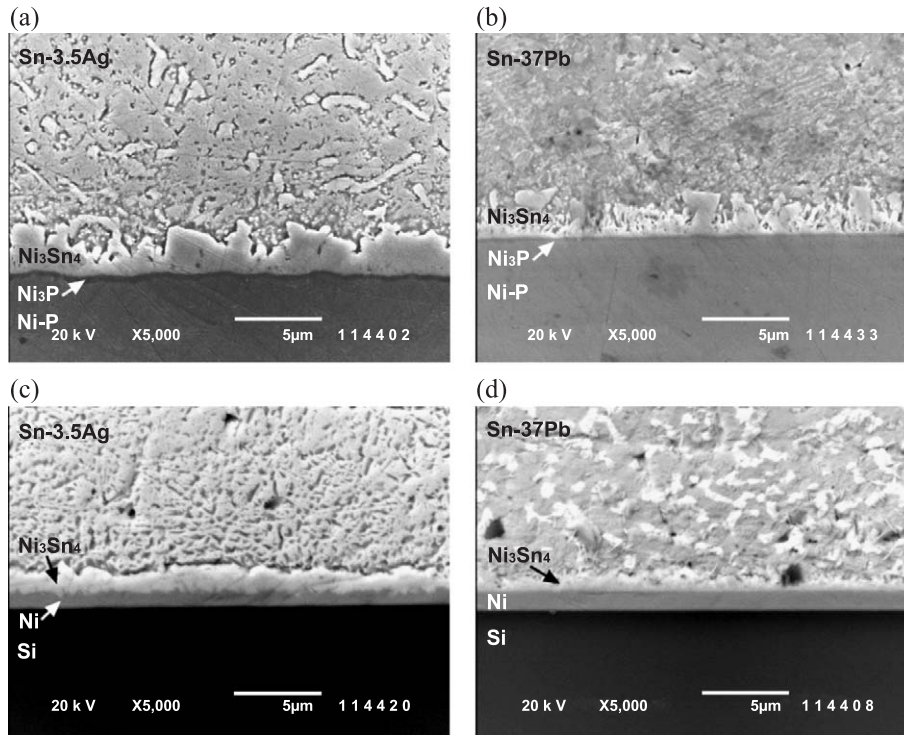


Fig. 1. Cross-sectional morphology of Ni₃Sn₄ in Sn-rich solders with Ni-based UBMs after reflow. (a) Sn–3.5Ag with Ni–P, (b) Sn–37Pb with Ni–P, (c) Sn–3.5Ag with sputtered Au/Ni, (d) Sn–37Pb with sputtered Au/Ni.

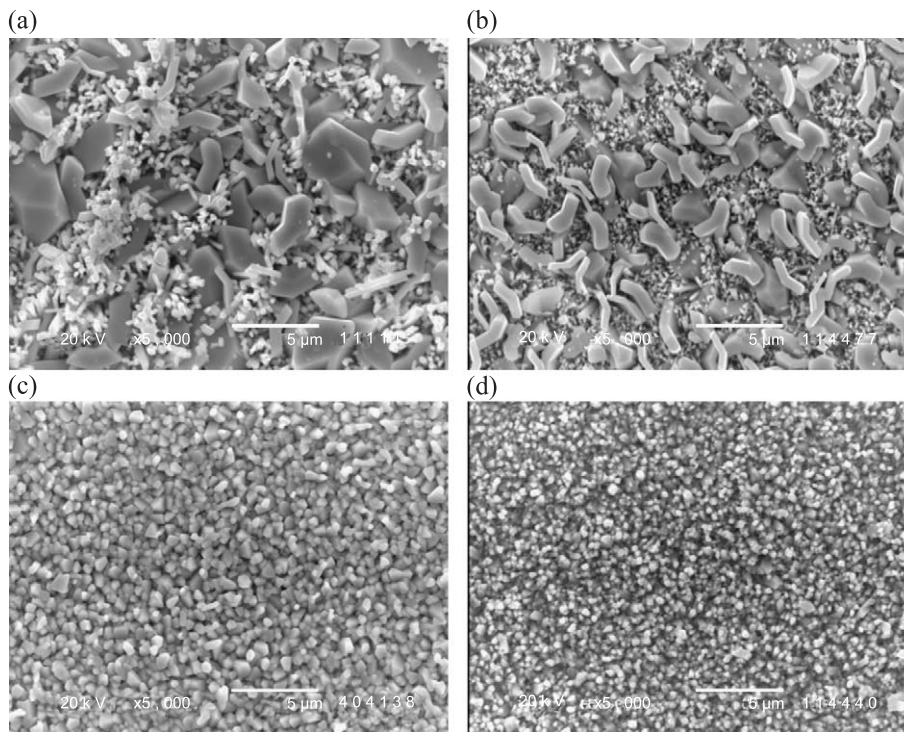


Fig. 2. Top structural morphology of Ni₃Sn₄ in Sn-rich solders with Ni-based UBMs after reflow. (a) Sn–3.5Ag with Ni–P, (b) Sn–37Pb with Ni–P, (c) Sn–3.5Ag with sputtered Au/Ni, (d) Sn–37Pb with sputtered Au/Ni.

2. Experimental procedures

The substrates used in this study were prepared from blank Si wafers. Si wafer was first sputtered with one layer of chromium in the thickness about 1000 Å, followed by sputter deposition of about 1 μm pure nickel and 0.3 μm gold. Ni–P (12.5 at.% P) UBM of about 5 μm was obtained by electroless plating using a commercial solution on the above mentioned sputtered nickel substrate. Before plating, the sputtered gold layer was etched away. A final finish of immersion gold on the plated Ni–P was applied as a surface protection. The sputtered Au/Ni was also used as a form of UBM to compare with the Ni–P UBM. Both the eutectic Sn–37Pb solder and Sn–3.5Ag solder used are in the form of wire with no-clean reflow flux in the core. The Sn–3.5Ag sample was heated to a peak temperature of 251 °C and kept at this temperature for 180 s, while eutectic Sn–37Pb was heated to and kept at 213 °C for 120 s. Selected Sn–3.5Ag solder samples were thermally aged at 130, 150, 170 and 190 °C for 100, 225, 400 and 625 h. Similarly, selected eutectic Sn–37Pb solder samples were thermally aged at 130, 150 and 170 °C for the same aging periods. Reflowed and aged samples were prepared for observations on cross-sectional and top structure (viewing from the solder phase towards the substrate after solder removal) of the IMC morphology at the solder/UBM interface. Common metallography practices were followed to reveal the cross-sectional microstructure. In order to observe the top view of the IMCs, the majority of the solder on the specimens was first ground away and the remaining solder was then etched with 2% HCl solution.

3. Results and discussion

3.1. Morphology of IMC

3.1.1. Morphology of IMC after reflow

The cross-sectional view of the interfacial microstructure developed from the four solder/UBM systems (Sn–3.5Ag and Sn–37Pb solders with the two Ni–P and sputtered Au/Ni UBMs) after reflow are shown in Fig. 1. Fig. 1a and b are SEM micrographs at the interface of the two solders with Ni–P UBM. The same interfacial IMC structure is observed: there exists a layer consisting of mainly Ni₃P crystals [13] sandwiched in between Ni₃Sn₄ and Ni–P, while Ni₃Sn₄ is in contact with the solidified solder. The Ni₃Sn₄ IMC layer in the Sn–3.5Ag/Ni–P system was observed to have needle-like and chunky grains and its average thickness is over 2 μm, intermetallics in the Sn–37Pb/Ni–P system have more needle-like spikes and the average thickness is around 1.3 μm. Fig. 1c and d are cross-sectional views of the interfacial microstructure of the two solders with sputtered Au/Ni UBM systems. From top to bottom, the regions in each of these micrographs are the solder, Ni₃Sn₄, Ni and Si, respectively. The interfaces

between the IMC and Ni film are relatively flat compared with the solder/Ni–P UBM combinations. In general, the IMC layer formed with sputtered Ni UBM is thinner than that with Ni–P UBM.

Fig. 2 shows the top structural micrographs of interfacial intermetallics for the four solder/UBM systems. The Ni₃Sn₄ IMCs formed by the two solders with electroless Ni–P UBM displayed a variety of grain sizes and shapes. Chunk-type, boomerang-type and needle-type Ni₃Sn₄ IMC morphology were observed, as shown in Fig. 2a and b. It was noticed that with the extension of reflow time these small needle grains were no longer present [14]. This suggests that these small grains are indeed formed during wetting reaction. Their disappearance may be attributed to ripening during wetting reaction. However, morphological differences of the IMCs between the two solder systems are

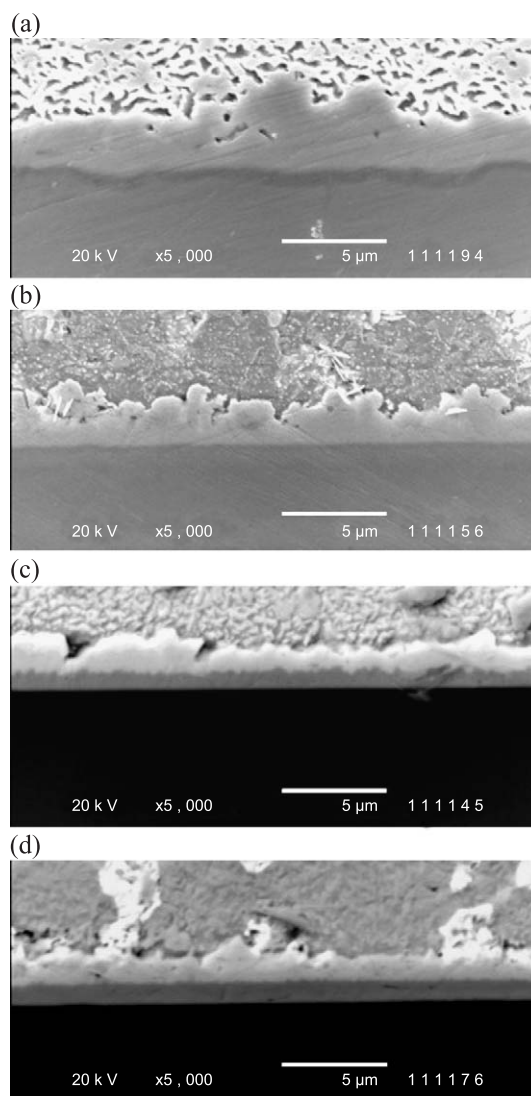


Fig. 3. Ni₃Sn₄ IMCs formed between solders and Ni-based UBMs after 100 h aging at 130 °C. (a) Sn–3.5Ag with Ni–P, (b) Sn–37Pb with Ni–P, (c) Sn–3.5Ag with sputtered Au/ Ni, (d) Sn–37Pb with sputtered Au/Ni.

appreciable. In the Sn–37Pb/Ni–P system, the amount and size of both boomerang-type and chunk-type IMC grains are much less than that of Sn–3.5Ag/Ni–P system. On the other hand, the IMCs formed on sputtered Au/Ni UBM are all scallop-type grains with faceted surfaces, and they have much smaller and more uniform grain sizes compared with Ni–P UBM system. Grain size in the Sn–37Pb solder system is also less than in the Sn–3.5Ag solder system with sputtered Au/Ni UBM.

Ni_3Sn_4 is the main intermetallic compound formed between the solder/UBM systems in Figs. 1 and 2, irrespective of its shape and sizes. This is in agreement with what was reported by other research groups [12–16]. Although P is not present in the IMC, it plays an important role in the formation and growth of the IMCs, which has been demonstrated from the clear difference in size and distribution of the IMCs formed in different systems. A notable difference between Ni–P and Ni UBMs is the formation of an additional layer of mainly crystalline Ni_3P , which is a result of Ni depletion and crystallization of the amorphous Ni–P phase in Ni–P UBM [7]. Ni_3P has very fine grains, 20 nm in grain size as mentioned by Liu et al. [17]. Our current work also observed fine Ni_3P grains of the size from 10 to 20 nm [18]. These fine grains structure may influence the diffusion of Ni by providing fast Ni diffusion channels in some particular locations. This could account for the different morphologies of Ni_3Sn_4 IMC in Ni–P UBM system.

3.1.2. IMC morphology evolution in solid state reaction

The solder reaction continues with time during the thermal aging process. This is evidenced by the morphology change and growth in thickness of the IMC layers as compared to the as-reflowed state. Typical cross-sectional interfacial microstructures of the four solder/UBM systems after aging are shown in Fig. 3 for short time at lower temperature, and in Fig. 4 for long time at higher temperature. It was observed that the top contour lines of the Ni_3Sn_4 layer become much flatter than as-reflowed samples. Such changes are more evident with the Sn–3.5Ag solder samples: the interface of the IMC layers with unconsumed amorphous Ni–P layer became more crooked (Figs. 3a and 4a), implying relatively more consumption of the Ni–P in certain locations with the growth of IMCs during thermal aging.

Typical top views of Ni_3Sn_4 IMCs in the four solder/UBM systems after aging are shown in Fig. 5. Only chunky Ni_3Sn_4 IMC grains with faceted surfaces are observed at the interface in these samples. The IMC grain sizes are much larger, and the surface appears less rough when compared to as-reflowed samples shown in Fig. 2. With the same UBM, the IMC grain sizes of Sn–3.5Ag solder joints are larger than those with Sn–Pb solder. For the same solder, Ni–P UBM results in larger IMC grains than pure Ni UBM.

A layer of Au–Ni–Sn ternary intermetallic is formed on the top of Ni_3Sn_4 layer in Sn–37Pb solder with Au/Ni UBM when aged at high temperatures for prolonged time, as

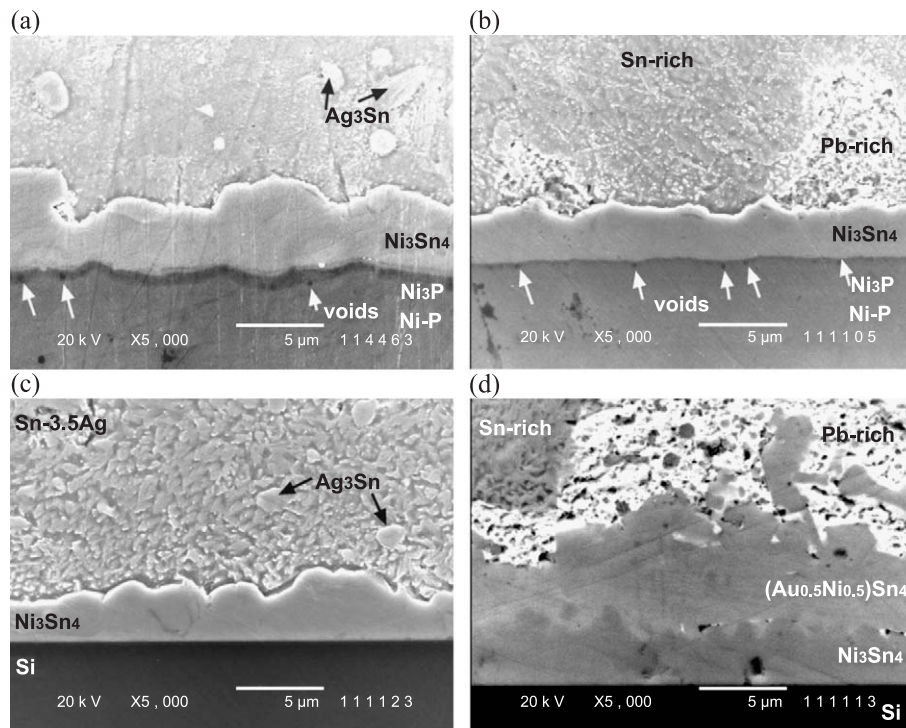


Fig. 4. Ni_3Sn_4 IMCs formed between solders and Ni-based UBMs after 625 h aging at 170 °C. (a) Sn–3.5Ag with Ni–P, (b) Sn–37Pb with Ni–P, (c) Sn–3.5Ag with sputtered Au/ Ni, (d) Sn–37Pb with sputtered Au/Ni.

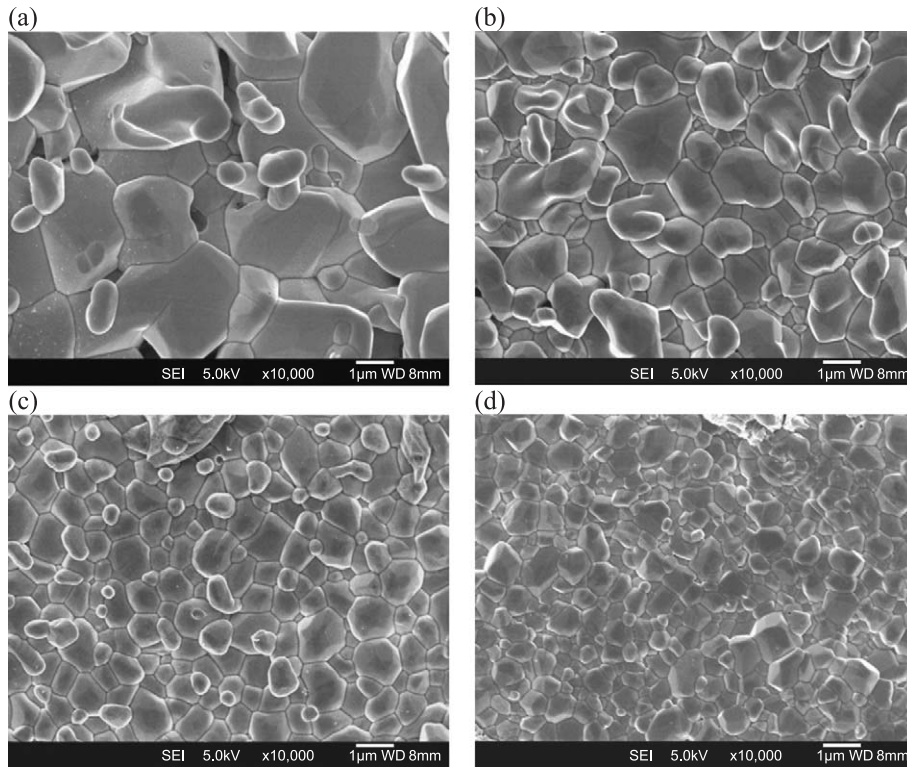


Fig. 5. Ni_3Sn_4 IMCs formed between solders and Ni-based UBMs after 400 h aging at 130 °C. (a) Sn–3.5Ag with Ni–P, (b) Sn–37Pb with Ni–P, (c) Sn–3.5Ag with sputtered Au/ Ni, (d) Sn–37Pb with sputtered Au/Ni.

shown in Fig. 4d. EDX analysis shows that the composition of this ternary IMC is close to $(\text{Au}_{0.5}\text{Ni}_{0.5})\text{Sn}_4$, which is in agreement with what has been reported by other researchers [12,16,19]. Thickness of $(\text{Au}_{0.5}\text{Ni}_{0.5})\text{Sn}_4$ layer is much greater than that of Ni_3Sn_4 . A Pb-rich layer is next to this Au–Ni–Sn ternary phase on the solder side. EDX line scanning, as shown in Fig. 6, indicates that the Pb-rich layer contains more Au than the $(\text{Au}_{0.5}\text{Ni}_{0.5})\text{Sn}_4$ phase. The presence of Pb in the SnPb solder is believed to play a role

in the formation of Au–Ni–Sn layer because the diffusivity of Au in Pb is about $10^{-9} \text{ cm}^2/\text{s}$, almost one order of magnitude faster than the diffusivity of Au in Sn [3]. The Pb-rich layer provides a fast diffusion path for Au to diffuse to the interface. In general, there is no continuous $(\text{Au}_{0.5}\text{Ni}_{0.5})\text{Sn}_4$ layer formed at the interface between Sn–3.5Ag solder and Au/Ni UBM. Elsewhere only dispersed $(\text{Au}_{0.5}\text{Ni}_{0.5})\text{Sn}_4$ intermetallics are seen inside the solder matrix and also at the outer surface of the solder ball.

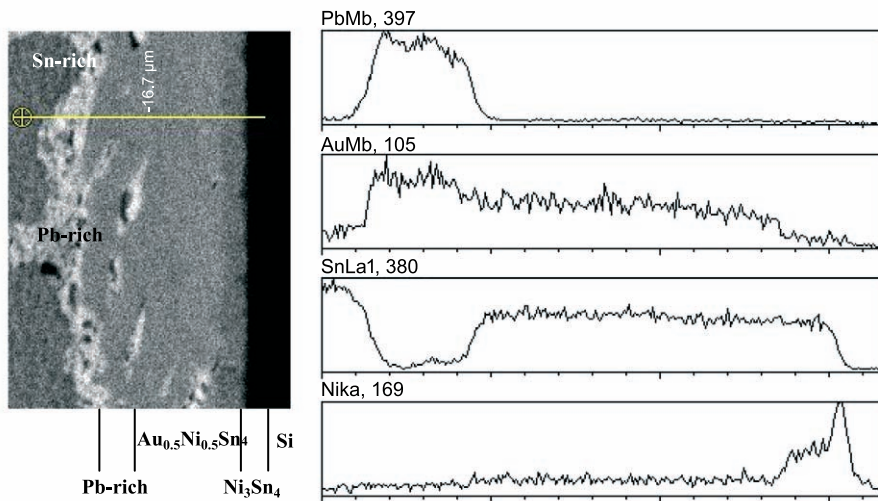


Fig. 6. EDX line scanning of the interfacial area at Sn–37Pb with Au/Ni UBM solder joint aged at 170 °C for 400 h.

3.2. Ni_3Sn_4 growth kinetics in solid state reaction

Ni_3Sn_4 IMC thickness of the four solder/UBM systems as a function of aging time and temperature is shown in Fig. 7. The IMC thickness increases linearly with square root of the aging time at a fixed aging temperature. This

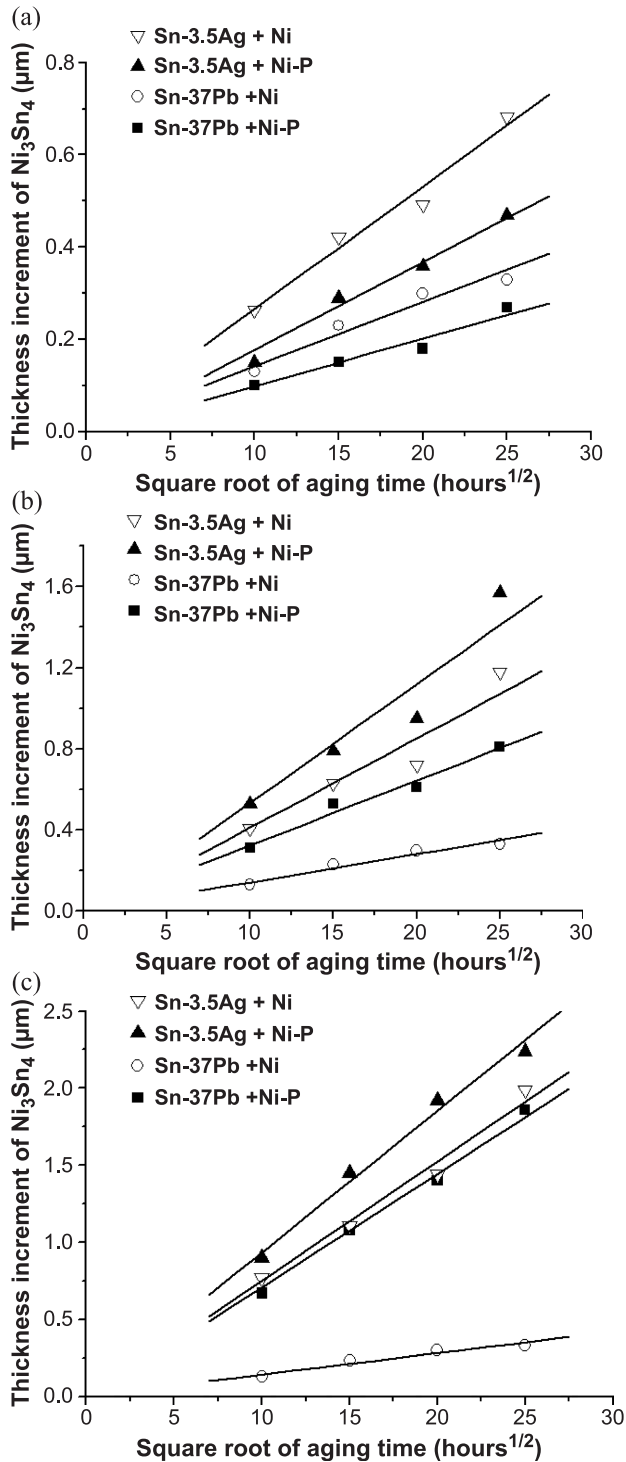


Fig. 7. Thickening kinetics of Ni_3Sn_4 layer in four sets of solder/UBM systems in solid state reaction. (a) 130 °C, (b) 150 °C, (c) 170 °C.

indicates that the IMC growth in all of the systems under discussion is a diffusion-controlled process. The growth rate constant at a particular temperature, k , can be calculated by the slope of the linear fitting lines.

In all four solder/UBM systems, IMC growth rate during thermal aging process increases with aging temperature. IMC grows faster with sputtered Au/Ni UBM than Ni-P UBM no matter which solder is used at the aging temperature of 130 °C. At higher temperatures (150 °C and above), IMC with Ni-P UBM shows faster growth than with sputtered Au/Ni UBM. A possible explanation for this may come from the grain size of Ni_3Sn_4 : the one formed on Ni-P UBM is much larger than that of sputtered Au/Ni UBM, as shown in Fig. 2. Smaller grains lead to more grain boundaries, which could be the dominant diffusion paths at low aging temperatures, resulting in faster IMC growth in the Au/Ni UBM systems. At higher temperatures, lattice diffusion becomes more significant than grain boundary diffusion. In addition, at relatively higher temperatures, the existence of Ni_3P phase could assist recrystallization of the amorphous Ni-P. The columnar fine grain structure of Ni_3P may assist nickel diffusion from Ni-P to the IMC phase [17].

At a fixed aging temperature, the thickness increment of IMC in Sn-3.5Ag solder systems is larger than that of SnPb solder with same UBM. In other words, Ni_3Sn_4 IMC in Sn-3.5Ag solder system grows faster than those in Sn-37Pb solder joints. The effect could come from the difference in diffusivity of certain elements in different solder phases. For example, in the Sn-Pb case, during the thermal aging process, the consumption of Sn to form Ni_3Sn_4 will result in an enrichment of Pb at the interface of solder and Ni_3Sn_4 IMC, as shown in Fig. 4b and d. The Pb-rich phase forms a barrier layer for Sn to continue the reaction with Ni, slowing down the overall reaction rate. And for SnPb solder with Au/Ni UBM, the formation of Pb-rich layer and $(\text{Au}_{0.5}\text{Ni}_{0.5})\text{Sn}_4$ IMC layer on Ni_3Sn_4 layer makes the further growth of Ni_3Sn_4 slower [19–21], even at the high aging temperature of 170 °C.

The variation of k with temperature can be represented by the Arrhenius equation

$$k = A \exp(-Q/RT) \quad (1)$$

where A is a prefactor, T the absolute temperature, R the gas constant and Q the effective activation energy of the reaction. An Arrhenius plot, as shown in Fig. 8, is obtained for Sn-3.5Ag solder with Ni-based UBM systems and Sn-37Pb solder with Ni-P UBM. The activation energy for the Ni_3Sn_4 growth in solid state reaction is estimated to be 110 kJ/mol for Sn-3.5Ag solder with Ni-P UBM and 91 kJ/mol for Sn-3.5Ag solder with sputtered Au/Ni UBM. Activation energy for Ni_3Sn_4 growth between Sn-37Pb solder and Ni-P UBM in solid state reaction is found to be 141 kJ/mol. For the same Sn-3.5Ag solder, the smaller Q value associated with the pure Ni UBM system indicates

the relative easiness in IMC growth in this system. And with the same Ni–P UBM, it needs to overcome higher activating energy for Ni_3Sn_4 to grow in eutectic Sn–Pb system than in Sn–3.5Ag system.

3.3. Kirkendall voids formation in Ni–P UBM system

Kirkendall voids were observed inside the Ni_3P layer from samples using both solders with Ni–P UBM. Typical views of such voids under SEM are shown in Fig. 4a and b. The existence of the SEM-observable voids and their number and sizes are dependent on the aging temperature and time. No voids are observable under SEM in samples aged at 130 °C for as long as 625 h. Voids can only be found after long period of aging at 150 °C for both solder systems. Fewer and smaller voids are observed with Sn–37Pb solder than with Sn–3.5Ag solder. The voids can be easily found in samples aged at higher temperatures for even a few hours, as shown in Fig. 9. Voids formed after only 9 h aging at 216 °C in Sn–3.5Ag solder and 100 h aging at 170 °C in SnPb solder.

The formation of Kirkendall voids inside the Ni_3P layer seems to be a phenomenon peculiar to samples with Ni–P UBM. No such voids are observed with pure Ni UBM. This suggests that the presence of the Ni_3P layer between the IMC and the UBM is a necessary condition for void formation. At the very beginning of solder reaction, the formation of Ni_3Sn_4 would deplete Ni from the surface of the electroless nickel alloy, resulting in crystallization of the P-enriched portion of the alloy to form Ni_3P [15]. During thermal aging process, the reaction between solder and UBM continues. Further supply of nickel for the Ni_3Sn_4 to grow may come from two sources, decomposition of Ni_3P at the reaction front or the diffusion of nickel from the unreacted Ni–P through the Ni_3P layer. Detailed discussion

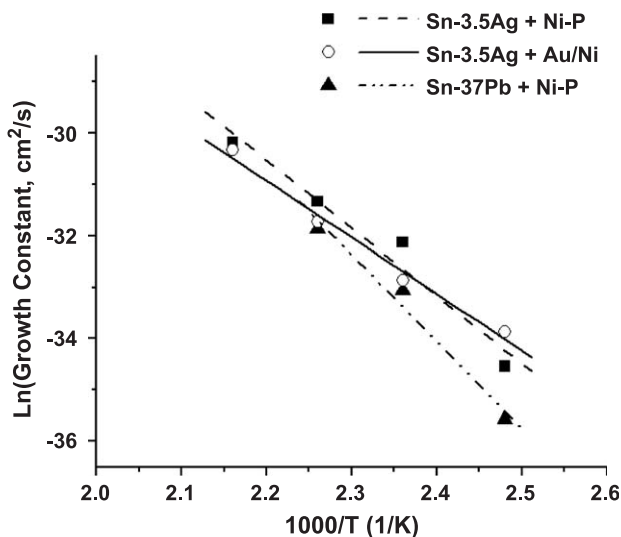


Fig. 8. Arrhenius plot for the formation of Ni_3Sn_4 IMC between Sn-rich solders and Ni-based UBMs.

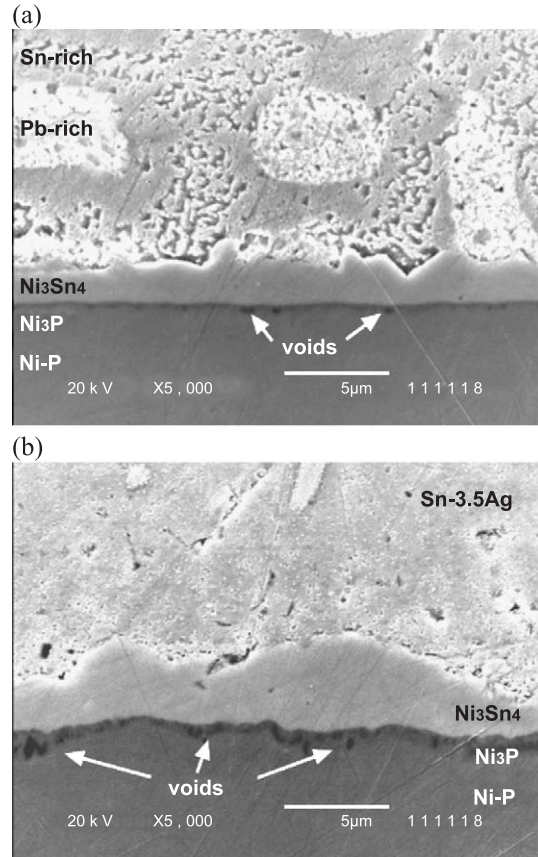


Fig. 9. Kirkendall voids formed inside Ni_3P layer at high temperature for short time aging. (a) Sn–37Pb solder aged at 170 °C for 100 h, (b) Sn–3.5Ag solder aged at 216 °C for 9 h.

was carried out elsewhere [18]. Current authors believe that for further growth of Ni_3Sn_4 , the provision of Ni must come from the unreacted Ni–P UBM layer. While Ni can diffuse through the Ni_3P layer easily, Sn is stopped because of the formation of an additional NiSnP layer [18] in between Ni_3Sn_4 and Ni_3P layers. This unbalanced diffusion causes the formation of the voids.

4. Conclusions

In this study, we have compared the morphologies and growth kinetics of intermetallic compounds formed between two types of Sn-rich solders (Sn–3.5Ag and eutectic Sn–Pb) and two types of Ni-based UBMs (electroless Ni–P and sputtered Au/Ni). On Ni–P UBM, the Ni_3Sn_4 IMCs formed by the Sn–3.5Ag solder exist in chunk-type, boomerang-type and needle-type crystal grains after reflow, while those formed by the eutectic Sn–Pb solder exhibit similar shapes but are of smaller size. With the sputtered Au/Ni UBM, Ni_3Sn_4 IMCs formed in the two solder systems appear in uniform fine crystals. Thermal aging results in an overall thickness increase and crystal grain size growth. The thickness of the IMC layers increases

linearly with the square root of the thermal aging time in all the solder/UBM combinations. With the same UBM, the IMC formed by eutectic Sn–Pb solder grows slower than that by Sn–3.5Ag solder. This is attributed to the formation of Pb-rich layer on the surface of Ni₃Sn₄ IMC encumbering the diffusion of Sn. Kirkendall voids are observed in samples of Ni–P UBM that have undergone long thermal aging treatment or which have been aged at high temperature. These voids are the result of unbalanced elemental diffusion at the interface between solder and the Ni–P UBM.

Acknowledgements

This work was supported by an Academic Research Fund from Nanyang Technological University. Helpful discussion with Prof. Andriy Gusak from Cherkasy National University, Ukraine is gratefully acknowledged.

References

- [1] E.P. Wood, K.L. Nimmo, *Journal of Electronic Materials* 23 (1994) 709.
- [2] S.J. Adamson, *Advanced Packaging* (2000) 46.
- [3] K. Zeng, K.N. Tu, *Materials Science and Engineering R38* (2002) 55.
- [4] K.N. Tu, K. Zeng, *Materials Science and Engineering R34* (2001) 1.
- [5] A.A. Liu, H.K. Kim, K.N. Tu, *Journal of Applied Physics* 80 (1996) 2774.
- [6] H.K. Kim, K.N. Tu, P.A. Totta, *Applied Physics Letters* 68 (1996) 2204.
- [7] P.L. Liu, J.K. Shang, *Metallurgical and Materials Transactions. A, Physical Metallurgy and Materials Science* 31A (2000) 2867.
- [8] Y.C. Chan, P.L. Tu, C.W. Tang, K.C. Hung, K.L. Lai, *IEEE Transactions on Advanced Packaging* 24 (2001) 25.
- [9] K.L. Lin, Y.C. Liu, *IEEE Transactions on Advanced Packaging* 22 (1999) 568.
- [10] Z. Mei, R.H. Dauskardt, *MRS Spring Meeting Symposium M, Materials Reliability in Microelectronics IX*, Materials Research Society (MRS), 1999, p. 1.
- [11] P.L. Liu, J.K. Shang, *Journal of Materials Research* 15 (2000) 2347.
- [12] C.E. Ho, W.T. Chen, C.R. Kao, *Journal of Electronic Materials* 30 (2001) 379.
- [13] J.W. Jang, D.R. Frear, T.Y. Lee, K.N. Tu, *Journal of Applied Physics* 88 (2000) 6359.
- [14] G.J. Qi, M. He, Z. Chen, *Proceedings of Yazawa International Symposium in Conjunction with the 132nd TMS Annual Meeting and Exhibition, March 2–6, 2003, San Diego, U.S.A., The Minerals, Metals & Materials Society, (TMS)*, 1, 2003, p. 1173.
- [15] J.W. Jang, P.G. Kim, K.N. Tu, D.R. Frear, P. Thompson, *Journal of Applied Physics* 85 (1999) 8456.
- [16] Y.D. Jeon, K.W. Paik, K.S. Bok, W.S. Choi, C.L. Cho, *Journal of Electronic Materials* 31 (2002) 520.
- [17] P.L. Liu, J.K. Shang, *Metallurgical and Materials Transactions. A, Physical Metallurgy and Materials Science* 31A (2000) 2857.
- [18] M. He, Z. Chen, G. Qi, *Acta Materialia* 52 (2004) 2047.
- [19] A.M. Minor, J.W. Morris, *Metallurgical and Materials Transactions. A, Physical Metallurgy and Materials Science* 31A (2000) 798.
- [20] K.Y. Lee, M. Li, *Metallurgical and Materials Transactions. A, Physical Metallurgy and Materials Science* 32A (2001) 2666.
- [21] C.M. Liu, C.E. Ho, W.T. Chen, C.R. Kao, *Journal of Electronic Materials* 30 (2001) 1152.